Carbohydrate Polymers 98 (2013) 914–921

Contents lists available at SciVerse ScienceDirect

Carbohydrate Polymers

journal homepage: www.elsevier.com/locate/carbpol

Comparison of xanthans by the relative abundance of its six constituent repeating units

Marijn M. Kool [a], Harry Gruppen [a], Graham Sworn [b], Henk A. Schols [a,*]

[a] Wageningen University, Laboratory of Food Chemistry, P.O. Box 8129, 6700 EV Wageningen, The Netherlands
[b] DUPONT, Danisco France SAS, 20 rue Brunel, 75017 Paris, France

ARTICLE INFO

Article history:
Received 7 May 2013
Received in revised form 13 June 2013
Accepted 2 July 2013
Available online 10 July 2013

Keywords:
Xanthan
HILIC–LC–MS
Cellulases
Substitution pattern
Acetyl groups

ABSTRACT

Five xanthans were hydrolyzed to their repeating units using cellulases. Hydrophilic interaction chromatography with online electrospray ionization ion trap mass spectrometry and evaporative light scattering detection was used to analyze the oligomers released. It was concluded that six different pentamer repeating units (RUs) exists within a xanthan sample. The most abundant RU shows acetylation on the inner mannose and pyruvylation on the outer mannose. The second most abundant RU shows acetylation on both the inner and the outer mannose. It becomes clear that more variations in the xanthan structure exist than generally recognized. Comparison of five different xanthan samples revealed that, although the molecular composition of xanthan samples can be exactly the same, the ratio in which the RUs occur can differ significantly. It is, therefore, concluded that xanthan samples should be characterized for both, their molecular composition and the relative abundance of the RUs present.

1. Introduction

Xanthan gum is an exopolysaccharide secreted by *Xanthomonas* spp. The generally accepted xanthan structure consists of a cellulosic backbone with trisaccharide side chains linked to every alternate glucose unit. These side chains consist of mannose–glucuronic acid–mannose units, which are substituted with an acetyl group on the inner mannose and a pyruvic acid ketal on the outer mannose (Jansson, Kenne, & Lindberg, 1975). The exact degree of substitution, however, is known to vary depending on the fermentation conditions (Flores Candia & Deckwer, 1999; Peters, Suh, Schumpe, & Deckwer, 1993) and the *Xanthomonas* strain used for xanthan production (Cadmus, Rogovin, Burton, Pittsley, Knutson, & Jeanes, 1976; Sutherland, 1981). The primary structure of the produced xanthan can be controlled by specific mutations in the *Xanthomonas* genome (Hassler & Doherty, 1990). Six different pentamer repeating units are proposed based on the genotype of the *Xanthomonas* strain used. It was shown that suppression of the gene involved in the pyruvylation of the outer mannose resulted in a higher degree of acetylation. It was therefore suggested that xanthan side chains can also be acetylated on the outer mannose. However the exact position of the acetyl groups was not determined. The six repeating units proposed by Hassler and Doherty were therefore only hypothesized and not experimentally determined. Another study also report on double acetylated side chains (Stankowski, Mueller, & Zeller, 1993). In this study sugar linkage analysis was used to determine the position of the second acetyl group. It was shown that acetylation on the *O*-6 position of the outer mannose, as proposed by Hassler and Doherty (1990), indeed occurs in xanthan molecules. About 24% of all outer mannose units are acetylated according to this study. However, the precise structure has not been linked to the individual repeating units and the ratio in which they coexist has not been determined.

To date, no conclusive study has been performed on the exact position of the acetyl groups in the xanthan side chains. The exact structure of the different xanthan repeating units present in one xanthan sample has, therefore, never been determined. In a previous study it is shown that cellulases can completely degrade xanthan to the xanthan repeating units (Kool et al., 2013). In the present study, these repeating units will be further characterized and used for quantification of the xanthan repeating units present in different xanthan samples. We thereby introduce a method that enables the unambiguous comparison of different xanthans.

2. Materials and methods

2.1. Xanthan samples

Five types of renatured xanthan were kindly provided by DuPont (Melle, France). The molecular compositions (Table 1) are determined as previously described (Kool et al., 2013). All samples have a molar glucose:mannose:glucuronic acid ratio which is close to the

* Corresponding author. Tel.: +31 317 482239; fax: +31 317 484893.
E-mail address: henk.schols@wur.nl (H.A. Schols).

0144-8617/$ – see front matter © 2013 Elsevier Ltd. All rights reserved.
http://dx.doi.org/10.1016/j.carbpol.2013.07.003

Table 1
Molecular composition of five xanthan samples.

Xanthan type	Glc:Man:GlcA molar ratio	Acetyl content (w/w%)	Pyruvate content (w/w%)
Xanthan A	1:0.88:0.41	5.6	4.4
Xanthan B	1:0.91:0.43	5.9	4.6
Xanthan C	1:0.92:0.44	4.9	5.1
Xanthan D	1:0.91:0.43	4.9	5.2
Xanthan E	1:0.94:0.45	4.8	7.3

expected ratio 2:2:1. The xanthan samples differ in their degree of substitution. Xanthans A and B show similar acetyl and pyruvyl contents of ~5.7% (w/w) and 4.5% (w/w), respectively. This corresponds to 1.15 acetyl and 0.56 pyruvyl groups per side chain, which indicates that the side chains can indeed be multiple acetylated. Xanthans C and D also have a similar composition to one another but have a slightly higher pyruvyl content and a slightly lower acetyl content compared to xanthans A and B. Xanthan E has a higher degree of pyruvylation, corresponding to almost fully pyruvylated side chains.

2.2. Enzymatic hydrolysis

Solutions containing 2 mg ml^{-1} xanthan were prepared in demineralized water and hydrolyzed using cellulases from the experimental enzyme preparation C1–G1 from *Myceliophtora thermophila C1* (Dyadic Netherlands, Wageningen, The Netherlands) (Kühnel, Schols, & Gruppen, 2011; Kool et al., 2013). The hydrolysis was performed by incubating 1 ml of a xanthan solution with 60 μg protein for 48 h at 60 °C. After incubation, the digests were boiled (10 min) and centrifuged (10,000 × *g*; 10 min; 25 °C). The supernatants were analyzed by HPSEC, HPAEC and UPLC–ELSD–MS^n.

2.3. High performance size exclusion chromatography (HPSEC)

HPSEC was performed as described previously (Kool et al., 2013). Molecular masses were estimated using pullulan molecular-mass standards (Polymer Laboratories, Palo Alto, CA, USA).

2.4. High performance anion exchange chromatography (HPAEC)

HPAEC was performed on an ICS5000 HPLC system (Dionex, Sunnyvale, CA, USA), equipped with a CarboPac PA-1 column (2 mm ID × 250 mm; Dionex) in combination with a CarboPac PA guard column (2 mm ID × 25 mm) and an ISC5000 ED PAD-detector (Dionex). The digests were centrifuged (10,000 × *g*; 10 min; 25 °C) and 2× diluted before injection onto the column (10 μl). Samples were eluted at a flow rate of 0.3 ml min^{-1} with the following elution profile of 0.1 M sodium hydroxide (NaOH) and 1 M sodium acetate (NaOAc) in 0.1 M NaOH: 0–10 min, 0–50 mM NaOAc in 0.1 M NaOH; 10–35 min, 50–400 mM NaOAc in 0.1 M NaOH; 35–40 min, 400–1000 mM NaOAc in 0.1 M NaOH; 40–45 min washing step with 1 M NaOAc in 0.1 M NaOH; 45–60 min, equilibration with 0.1 M NaOH. The glucose released was quantified based on the response factor of standard D-glucose.

2.5. Hydrophilic interaction liquid chromatography with evaporative light scattering and mass spectrometry detection (HILIC–ELSD–MS)

Digests were analyzed using UPLC–ELSD–MS^n on a HILIC BEH amide column (Waters Corporation, Milford, MA, USA) as described elsewhere (Leijdekkers, Sanders, Schols, & Gruppen, 2011) with a modified gradient. The following elution profile was used, with (A) 1% (v/v) acetonitrile (ACN) in water; (B) 100% ACN; and (C) 2% (v/v) formic acid in 200 mM ammonium formate solution: 0–1 min, isocratic 15% A, 80% B and 5% C; 1–25 min, linear to 45% A, 50% B and 5% C; 25–30 min linear to 55% A, 40% B and 5% C; 30–35 min, isocratic 55% A, 40% B and 5% C; 35–35.1 min linear to 15% A, 80% B and 5% C; 35.1–40 min, isocratic 15% A, 80% B and 5%. The xanthan digests were centrifuged and diluted 1:1 with ACN before injection (5 μl) into the system. The Acquity BEH Amide column was coupled to a splitter (Accurate, Dionex Corporation) directing the eluent to an ELSD and to an ESI–MS^n-detector with a ratio 10:1, respectively. The ELSD micro flow nebulizer (Sedere, France) had a gas pressure of 3.5 bar and a gas flow of 1.75 L min^{-1}. The drift tube temperature of the ELSD was set to 50 °C and the gain to 12. MS-detection was performed in negative mode on a Velos Pro ion trap MS (Thermo Scientific, San Jose, CA, USA) with the ion source voltage set to −4.5 kV, capillary temperature 250 °C, sheath gas 30 (arbitrary units), auxiliary gas 12 (arbitrary units). Mass spectra were acquired over the scan range *m*/*z* 300–2000. MS^n-collection parameters included normalized collision energy 35 (arbitrary units), activation Q 0.25 (arbitrary units), activation time 30 ms and isolation width 2 *m*/*z*.

3. Results and discussion

3.1. Enzymatic hydrolysis of the xanthan backbone

The different xanthans were incubated with cellulases in order to completely degrade the xanthans into their repeating units. In a previous study we showed that cellulases from the C1–G1 preparation from *Myceliophthora thermophila C1* can completely hydrolyze the xanthan backbone when xanthan is present in a completely disordered conformation (Kool et al., 2013). To ensure that the different xanthans were indeed completely hydrolyzed at the incubation conditions chosen, HPSEC was used to determine the molecular weight distribution of the xanthan digests (Fig. 1). After a 48 h incubation all xanthan samples are indeed completely hydrolyzed to xanthan oligosaccharides. The xanthan degradation products can, therefore, be used for quantification and characterization.

3.2. Analysis of xanthan degradation products using HPAEC

As HPAEC is a common method for mono- and oligosaccharide analysis (Hardy & Rohrer, 2007), the xanthan digests were analyzed by HPAEC (Fig. 2). Small amounts of glucose were released (≤5% of all glucose) in all digests, while release of mannose and/or glucuronic acid was not observed. It is, therefore, concluded that the cellulases used do not show any side chain degrading activity. The free glucose could originate from parts of the backbone where the side chain is lacking (Sutherland, 1984), enabling the cellulases to release glucose.

Next to the release of glucose, two additional peaks are observed in the HPAEC elution patterns. Because HPAEC is conducted under alkali conditions, acetyl esters originally present will be saponified online. The two peaks will, therefore, represent: (1) the unsubstituted pentamer RU and (2) the pyruvylated pentamer RU. Because side chains carrying a pyruvic acid acetal are more negatively charged than unsubstituted side chains, the pyruvylated RU elutes later, as was confirmed by the analysis of a pyruvate free xanthan

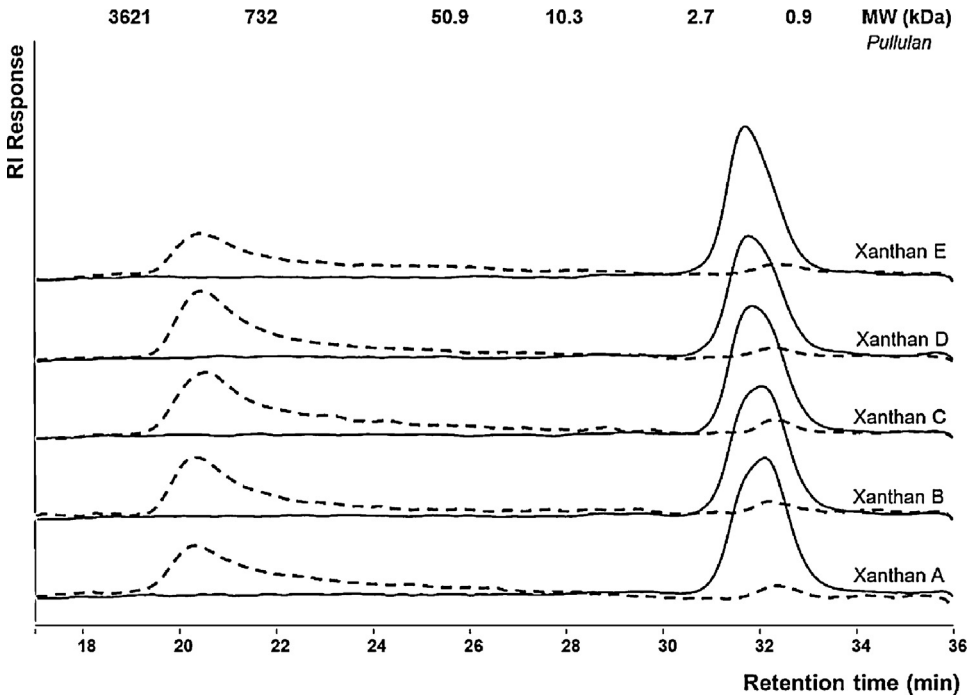

Fig. 1. HPSEC elution patterns of xanthan digests obtained after 48 h of incubation at 60 °C (solid line), and the corresponding xanthan blanks (dotted line).

(results not shown). No other degradation products are observed in the HPAEC elution pattern of any of the xanthan digests. Therefore, we conclude that under the chosen enzyme conditions, all xanthans are completely degraded to the xanthan RUs, confirming the HPSEC results.

3.3. Characterization of xanthan repeating units using LC–MS

No information on the position of acetyl groups can be obtained by HPAEC due to the online saponification of the acetyl esters. The xanthan repeating units (RUs) were, therefore, further characterized using hydrophilic liquid interaction chromatography (HILIC) with online mass spectrometry (MS).

The HILIC elution pattern of the xanthan A digest (Fig. 3) shows that the different RUs present in the cellulase digest are well separated. Five different peaks are recognized. The broad peaks are a results of partial α-/β-anomer separation, as was also observed for maltodextrins using the same column (Leijdekkers et al., 2011).

Electrospray ionization ion trap mass spectrometry (ESI–IT–MS^n) was used to identify all five compounds. The dominant peak (peak 3) has a *m*/*z*-value of 953, corresponding to the negative ion of the RU that is both pyruvylated and acetylated. Fig. 4 shows the fragmentation pattern of this RU, according to the nomenclature described by Domon and Costello (1988). The most abundant fragments are *m*/*z* 909, 791 and 703, which were interpreted as follows: *m*/*z* 909 (953-44, loss of a carboxyl group), 791 (953-162, loss of a glucose unit) and 703 (953-250, loss of pyruvylated mannose). The fragment *m*/*z* 541 can be annotated as the RU without 2 hexoses and a pyruvyl group. This mass loss can only be explained when one glucose is cleaved simultaneously with the pyruvylated outer mannose. Such double cleavage, from both sides of an oligosaccharides, has been reported previously in

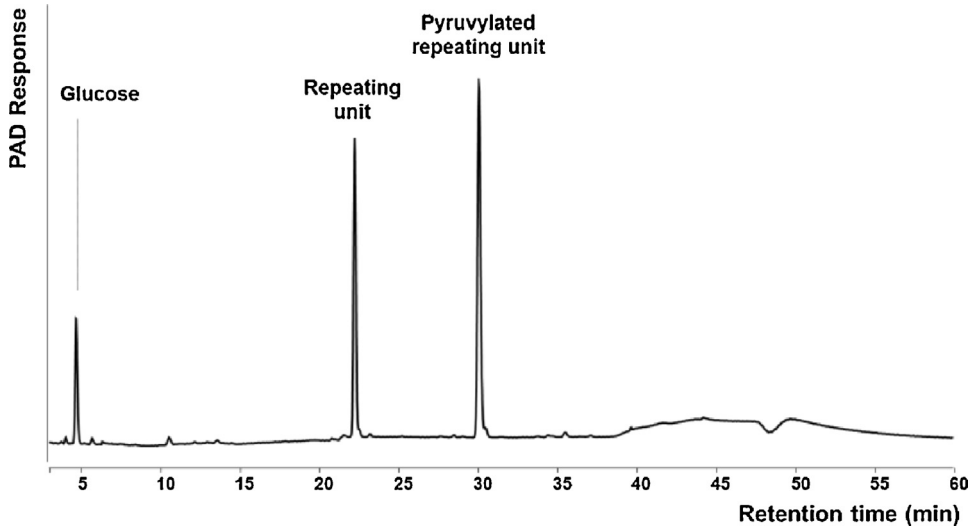

Fig. 2. HPAEC elution pattern of the 48 h xanthan A cellulase digest.

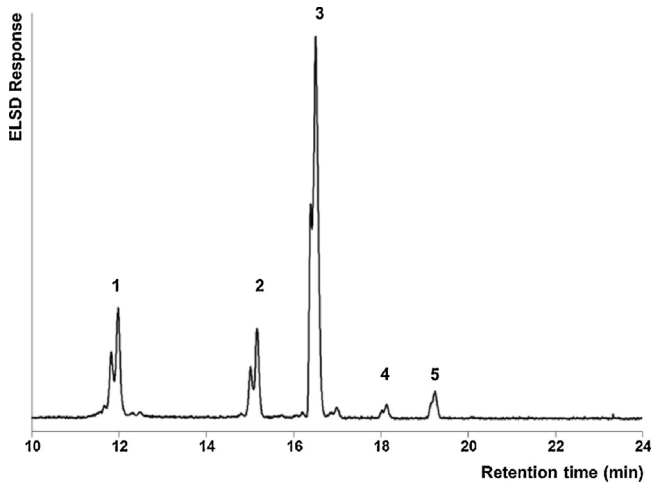

Fig. 3. HILIC ELSD elution pattern of the 48 h xanthan A cellulase digest.

the fragmentation pattern of xyloglucan oligomers (Hilz, de Jong, Kabel, Schols, & Voragen, 2006).

Table 2 shows the *m*/*z*-values and the fragmentation patterns of all compounds in the xanthan A digest. Considering the double cleavage observed in the fragmentation pattern of the acetylated and pyruvylated RU, all compounds could be identified as xanthan pentamer RUs differing in substitution pattern. Peak 1 (Fig. 3) has a *m*/*z*-value of 925, which corresponds to the negative ion of a RU that is substituted with two acetyl groups. The MS-fragmentation shows that one acetyl group is positioned on the inner mannose and the other on the outer mannose, as was previously shown by Stankowski et al. (1993) using linkage analysis. Peak 2 has a *m*/*z*-value of 883, which corresponds to the negative ion of a single acetylated RU. Fig. 5 shows the fragmentation pattern of this RU and the structures of the two possible acetylated RUs. The most abundant fragments are *m*/*z* 721, 703 and 541, which were interpreted as follows: 721 (883-162, loss of a glucose), 703 (883-180, loss of a mannose unit) and 541 (883-342, loss of a glucose and mannose unit). The loss of unsubstituted mannose is indicative for acetylation on the inner mannose. Fragments *m*/*z* 661 and 499 were interpreted as follows: *m*/*z* 661 (883-222, loss of an acetylated mannose unit) and 499 (883-384, loss of an acetylated mannose and a glucose unit). These fragments are thereby specific for acetylation on the outer mannose. The fragmentation pattern of peak 2 is, therefore, indicative for the presence of two different single acetylated repeating units. Based on the relative abundance of the specific *m*/*z* fragments, it can be concluded that most of the single acetylated RUs are acetylated on the inner mannose (≤85%).

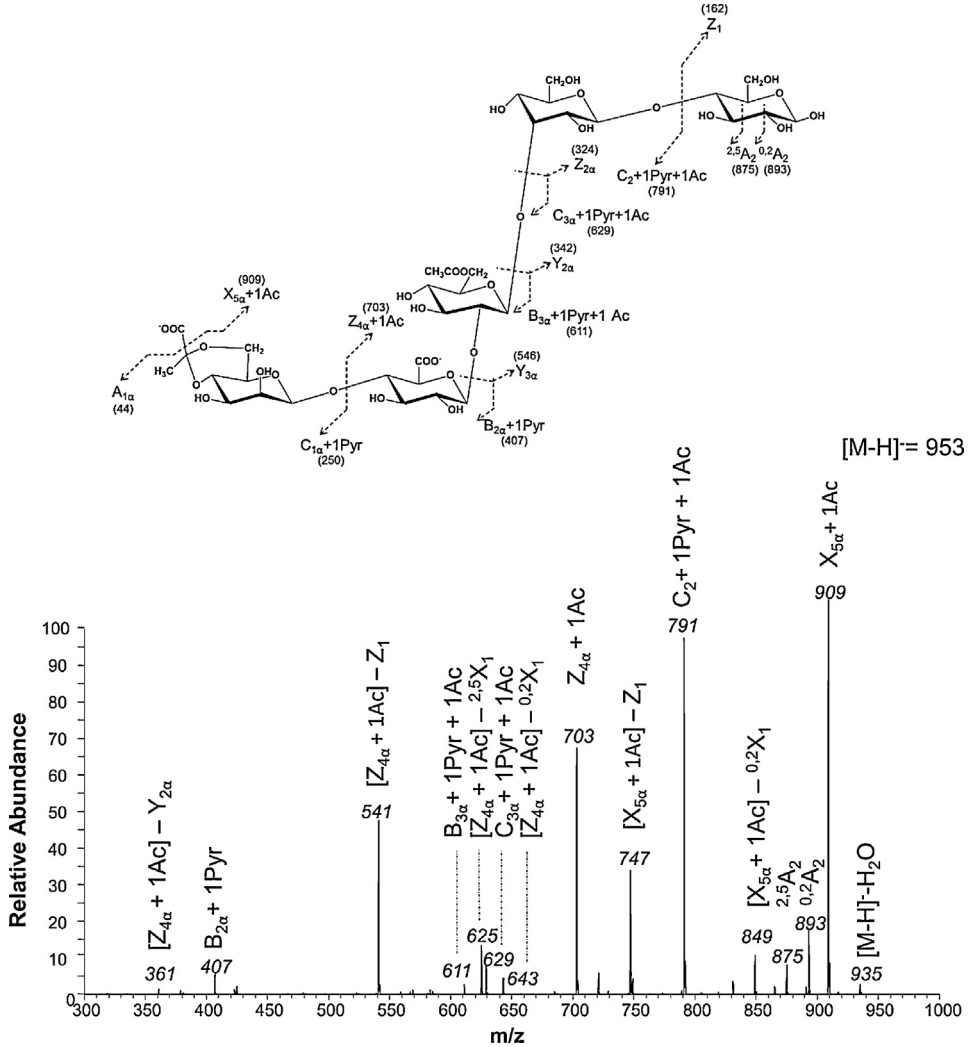

Fig. 4. MS^2 fragmentation pattern of the acetylated and pyruvylated pentamer repeating unit, eluting at 16.5 min in Fig. 3 and the chemical structure of *m*/*z* 953 with the observed cleavages according to the nomenclature of Domon and Costello (1988).

Table 2
Fragmentation pattern and identification of the peaks in Fig. 3 according to the nomenclature of Domon and Costello (1988) as depicted in Fig. 4.

Peak number	RT (min)	$[M-H]^-$ (*m/z*)	Ion fragments (*m/z*)	Proposed structure	Structure code
1	11.7–12.3	925	**907** ($[M-H]^-$-H_2O), **865** ($[M-H]^-$-$^{0,2}X_1$), **847** ($[M-H]^-$-$^{2,5}X_1$), **763** ($[M-H]^-$-Glc), **703** ($[M-H]^-$-AcMan), **625** ($[M-H]^-$-$^{2,5}X_1$; -AcMan), **541** ($[M-H]^-$-Glc; -AcMan), **379** ($[M-H]^-$-Glc-Glc-AcMan), **361** ($[M-H]^-$-Glc-Glc; -AcMan)		RU-1
2	14.9–15.3	883	**823** ($[M-H]^-$-$^{0,2}X_1$), **805** ($[M-H]^-$-$^{2,5}X_1$), **721**($[M-H]^-$-Glc), **703**($[M-H]^-$-Man), **643** ($[M-H]^-$-$^{0,2}X_1$; -Man), **625** ($[M-H]^-$-$^{2,5}X_1$; -Man), **541** ($[M-H]^-$-Glc; -Man), **361** ($[M-H]^-$-Glc-Glc;-Man)		RU-2
			823 ($[M-H]^-$-$^{0,2}X_1$), **805** ($[M-H]^-$-$^{2,5}X_1$), **721** ($[M-H]^-$-Glc), **661** ($[M-H]^-$-AcMan), **601** ($[M-H]^-$-$^{0,2}X_1$; -AcMan), **583** ($[M-H]^-$-$^{2,5}X_1$; -AcMan), **499** ($[M-H]^-$-Glc; -AcMan), **379** ($[M-H]^-$-Glc-Glc-Man)		RU-3
3	16.3–16.7	953	**909** ($[M-H]^-$-CO_2), **893** ($[M-H]^-$-$^{0,2}X_1$), **849** ($[M-H]$-CO_2; -$^{0,2}X_1$), **791** ($[M-H]^-$-Glc), **747** ($[M-H]$–Glc; -CO_2), **703** ($[M-H]^-$-PyrMan), **625** ($[M-H]^-$-$^{2,5}X_1$; -PyrMan), **541** ($[M-H]^-$-Glc; -PyrMan), **407** ($[M-H]^-$-Glc-Glc-AcMan), **361** ($[M-H]^-$-Glc-Glc; -PyrMan)		RU-4
4	18.0–18.3	841	**781** ($[M-H]^-$-$^{0,2}X_1$), **763** ($[M-H]^-$-$^{2,5}X_1$), **679** ($[M-H]^-$-Glc), **661** ($[M-H]^-$-Man), **601** ($[M-H]^-$-$^{0,2}X_1$; -Man), **517** ($[M-H]^-$-Glc-Glc), **499** ($[M-H]^-$-Glc; -Man)		RU-5
5	19.1–19.4	911	**967** ($[M-H]^-$-CO_2), **851** ($[M-H]^-$-$^{0,2}X_1$), **807** ($[M-H]^-$-CO_2; -$^{0,2}X_1$), **749** ($[M-H]^-$-Glc), **705** ($[M-H]^-$-Glc; -CO_2), **661** ($[M-H]^-$-PyrMan), **601** ($[M-H]^-$-$^{0,2}X_1$; -PyrMan), **583** ($[M-H]^-$-$^{2,5}X_1$; -PyrMan), **569** ($[M-H]^-$-Glc-Glc), **499** ($[M-H]^-$-Glc; -PyrMan), **407** ($[M-H]^-$-Glc-Glc-Man)		RU-6

(●) glucose; (●) mannose; (◪) glucuronic acid; (○) acetyl groups; (●) pyruvic acid acetal

Peaks 4 and 5 in the HILIC elution pattern (Fig. 3) can be identified as the unsubstituted xanthan RU and the non-acetylated, but pyruvylated RU, respectively. In total six different pentamer RUs are identified. Thereby we confirm that the RUs proposed by Hassler and Doherty (1990) are indeed present in xanthan. However, these authors suggested that some RUs are only synthesized after specific mutations in the DNA of *Xanthomonas* and that native *Xanthomonas* strains would only express RUs that are substituted on both the inner and outer mannose. In this study it is now shown that all six repeating units can coexist in one xanthan sample, even when the *Xanthomonas* strain is not genetically modified. Therefore, it is concluded that '*the*' xanthan repeating unit does not exist and that the xanthan structure is much more complex than generally depicted in the literature. Whether the presence and abundance of the different RUs are resulting from irregularities in the biosynthesis or originate from the downstream processing of xanthan during production remains uncertain.

3.4. Relative abundance of the xanthan repeating units in different xanthan samples based on UPLC–ELSD response

Now that it is shown that the position of the acetyl group can vary, xanthan samples with the same levels of acetylation and pyruvylation may still differ in the relative abundance of the RUs present. The five xanthan samples were, therefore, also compared based on the RUs present in their cellulase digests.

HILIC elution patterns of the different cellulase digests showed that every type of xanthan contained all six RUs (results not shown). Because no suitable standards were available, the ratio in which the RUs are present in the xanthan samples was determined based on the ELSD-response, as a previous study showed that the ELSD response of different types of oligosaccharides is similar (Remoroza et al., 2012). Because the two isomeric single acetylated RUs elute simultaneously, the MS fragmentation pattern was used to determine the ratio in which these RUs are present.

Table 3 gives an overview of the relative abundance of the RUs present in the xanthan samples. The most abundant RU in all xanthan types is RU-4, which is acetylated on the inner mannose and pyruvylated on the outer mannose. Depending on the type of xanthan, the second most abundant repeating unit in xanthan is the double acetylated repeating unit (RU-1), the repeating unit acetylated on the inner mannose (RU-2) or the pyruvylated repeating unit (RU-6). Together the two double substituted side chains typically represent about 79% of all xanthan side chains, independent of the xanthan type. The results, therefore, indicate that

Table 3
Relative abundance (mol%) of the repeating units in different xanthan samples based on the ELSD-response after HILIC separation of 48 h cellulase digests.

Xanthan type	RU-1 	RU-2 	RU-3 	RU-4 	RU-5 	RU-6 	Substitution outer mannose (%)	Substitution inner mannose (%)	% of all acetyl groups on outer mannose	Double substituted RUs (%)	Ac:Pyr-ratio on the outer mannose
Xanthan A	19	10	2	62	3	4	87	91	19	81	1:3.2
Xanthan B	17	11	1	61	3	7	86	89	14	78	1:3.8
Xanthan C	4	12	1	75	2	6	86	91	5	79	1:16.2
Xanthan D	10	8	0	64	3	15	89	82	11	74	1:7.9
Xanthan E	5	3	1	73	3	15	94	81	6	78	1:14.7

(●) glucose; (●) mannose; (◪) glucuronic acid; (○) acetyl groups; (●) pyruvic acid ketal.

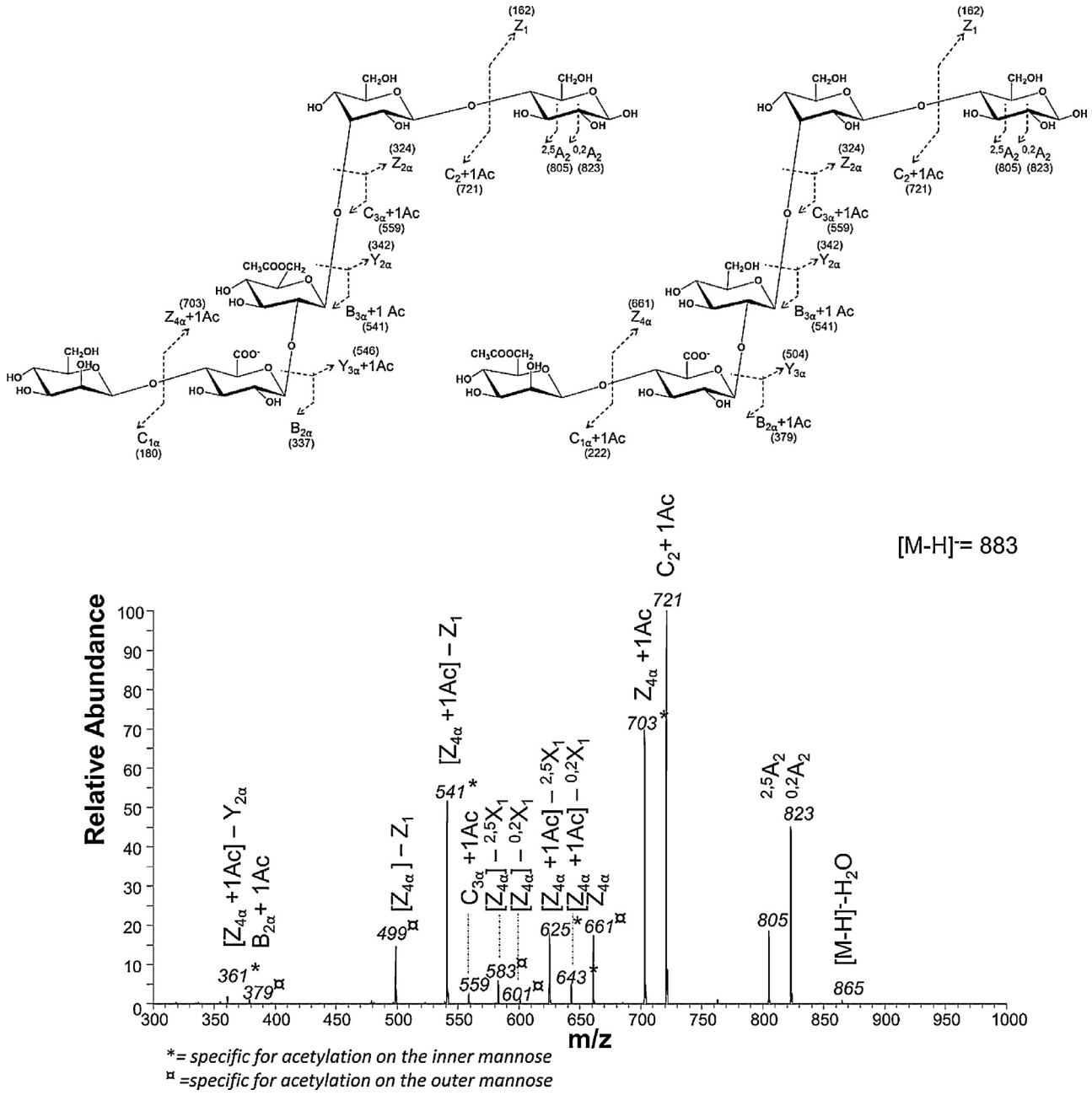

Fig. 5. MS^2 fragmentation pattern of the single acetylated pentamer repeating unit, eluting at 15.1 min in Fig. 3 and the two isomeric chemical structures of *m/z* 883 with the observed cleavages according to the nomenclature of Domon and Costello (1988).

independent of the conditions used during the xanthan production, approximately the same amount of double substituted side chains are present.

The influence of the production conditions on the biosynthesis of xanthan and the degree of pyruvylation of the xanthan produced has been described in various studies. A deficiency of nitrogen during the fermentation increases the pyruvate content, whereas a deficiency of oxygen decreases the pyruvate content (Flores Candia & Deckwer, 1999; Flores, Torres, & Galindo, 1994; Peters, Suh, Schumpe, & Deckwer, 1993). Furthermore it is known that the presence of citric acid in the growth media results in a xanthan with a high pyruvate level (Jana & Ghosh, 1999) and limitations of the amount of magnesium or phosphate in the growth media results in a xanthan with low pyruvate levels (Davidson, 1978). In most of these studies, however, the effect of the fermentation conditions on the level of acetylation was not studied. This study shows that there is no clear correlation between the fermentation conditions and the *total* amount of double substituted side chains synthesized However, a correlation between fermentation conditions and the acetyl:pyruvyl-ratio on the outer mannose is observed. We therefore propose that suppression of the biosynthesis of a pyruvate group on the outer mannose, by selective fermentation conditions, results in higher levels of acetylation on the outer mannose. This is in alignment with Davidson (1978) who observed an increase in the total acetyl content with decreasing pyruvate content. It also aligns with results found by Hassler and Doherty (1990) which showed that blocking the ketalase activity through mutations in gene L, results in the production of xanthan with high acetyl levels. In total 5–19% of all acetyl groups are positioned on the outer mannose, while Stankowski et al. (1993) mentioned

values of 20–25% for their xanthan based on sugar linkage analysis. No clear correlation is observed between the acetylation of the inner mannose and the substitution on the outer mannose.

3.5. Differentiation between 'similar' xanthans based on their repeating units

Comparison of the molecular composition of the different xanthans (Table 1) showed that xanthan C and D are almost identical. However, Table 3 illustrates the existence of differences between these xanthans. Xanthan D has twice as much RU-6, which is only substituted with a pyruvate group on the outer mannose, than xanthan C, whereas xanthan C has higher levels of RU-4. Furthermore, xanthan D has higher levels of the double acetylated RU, whereas xanthan C has more single acetylated RUs (RU-2 and RU-3). Thereby, xanthan C has a slightly higher degree of substitution on the inner mannose and a slightly lower degree of substitution on the outer mannose compared to Xanthan D. Cross analysis of the acetyl and pyruvate content of the xanthans (Table 1) corresponds rather well with the acetyl and pyruvate levels calculated from the type and relative abundance of the repeating units. It can, therefore, be concluded that two xanthans similar in molecular composition, may significantly differ in their structure. Establishing these differences in the structure of xanthans, may help to explain differences in functionality between two xanthans with the same molecular composition.

3.6. Impact of new findings

The effect of acetyl and pyruvate groups on the functionality of xanthan is widely discussed in the literature and conclusions are generally based on the quantitative analysis of the substituents. The influence of the exact distribution of the substituents on the functionality of xanthan, however, has been largely ignored in functionality studies due to the assumption that the xanthan substitution pattern is close to the idealized repeating unit.

Some studies show that acetyl and/or pyruvyl groups do not influence the xanthans functionality (Callet, Milas, & Rinaudo, 1987; Shatwell, Sutherland, & Ross-Murphy, 1990). However, most studies show that acetyl groups stabilize the xanthan conformation, reduce the interaction with galactomannans and reduce the xanthan viscosity, while pyruvyl group have the reversed effect (Morrison, Clark, Talashek, & Yuan, 2004; Renou, Petibon, Malhiac, & Grisel, 2013; Smith, Symes, Lawson, & Morris, 1984). The effect of acetyl groups is attributed to increased association of the side chains with the backbone, due to hydrogen bonding between the xanthan backbone and the acetyl groups on the inner mannose (Morris, Rees, & Young, 1977; Pelletier, Viebke, Meadows, & Williams, 2001; Tako & Nakamura, 1984).

Our study shows that the substitution pattern within the xanthan side chains is different than generally assumed and varies between xanthan samples. It is therefore likely that the relative abundance of the different RUs needs to be taken into account when studying the effect of the substituents on xanthan's functionality, especially regarding the substitution of the outer mannose unit. Because it is now shown that about 11% of all acetyl groups are positioned on the outer mannose, conclusions on the effect of acetyl groups on xanthans functionality should be reconsidered.

4. Conclusions

In this research an analytical method is introduced to characterize and compare xanthan samples. The unambiguous identification and quantification of six different RUs, demonstrate that substitution on the outer mannose unit is much more abundant than generally assumed. In addition to the 66–88% of the outer mannose units that are pyruvylated, 5–21% of the outer mannose units are acetylated. Comparison of different xanthans showed that the ratio in which the six repeating units are present, differs between xanthan samples even when the molecular composition is similar. It is, therefore, concluded that the characterization of xanthan samples should include the relative abundance of the RUs present, as well as the molecular composition of a xanthan sample.

Acknowledgments

This research was supported by the European Community within a consortium PolyModE KBBE-2007-3-3-07 and is gratefully acknowledged.

References

Cadmus, M. C., Rogovin, S. P., Burton, K. A., Pittsley, J. E., Knutson, C. A., & Jeanes, A. (1976). Colonial variation in *Xanthomonas campestris* NRRL B-1459 and characterization of the polysaccharide from a variant strain. *Canadian Journal of Microbiology*, *22*(7), 942–948.

Callet, F., Milas, M., & Rinaudo, M. (1987). Influence of acetyl and pyruvate content on rheologyical properties of xanthan in dilute solution. *International Journal of Biological Macromolecules*, *9*(5), 291–293.

Davidson, I. W. (1978). Production of polysaccharide by *Xanthomonas campestris* in continuous culture. *FEMS Microbiology Letters*, *3*(6), 347–349.

Domon, B., & Costello, C. E. (1988). A systematic nomenclature for carbohydrate fragmentations in FAB–MS/MS spectra of glycoconjugates. *Glycoconjugate Journal*, *5*(4), 397–409.

Flores Candia, J. L., & Deckwer, W. D. (1999). Effect of the nitrogen source on pyruvate content and rheological properties of xanthan. *Biotechnology Progress*, *15*(3), 446–452.

Flores, F., Torres, L. G., & Galindo, E. (1994). Effect of the dissolved oxygen tension during cultivation of *X. campestris* on the production and quality of xanthan gum. *Journal of Biotechnology*, *34*(2), 165–173.

Hardy, M. R., & Rohrer, J. S. (2007). High-pH anion-exchange chromatography (HPAEC) and pulsed amperometric detection (PAD) for carbohydrate analysis. In J. P. Kamerling, G. J. Boons, Y. C. Lee, A. Suzuki, N. Taniguchi, & F. Voragen (Eds.), *Comprehensive glycoscience: From chemistry to systems biology* (pp. 303–324). Elsevier Ltd.

Hassler, R. A., & Doherty, D. H. (1990). Genetic engineering of polysaccharide structure: Production of variants of xanthan gum in *Xanthomonas campestris*. *Biotechnology Progress*, *6*(3), 182–187.

Hilz, H., de Jong, L. E., Kabel, M. A., Schols, H. A., & Voragen, A. G. J. (2006). A comparison of liquid chromatography, capillary electrophoresis, and mass spectrometry methods to determine xyloglucan structures in black currants. *Journal of Chromatography A*, *1133*(1/2), 275–286.

Jana, A. K., & Ghosh, P. (1999). Effect of citric acid on the biosynthesis and composition of xanthan. *Journal of General and Applied Microbiology*, *45*, 115–120.

Jansson, P. E., Kenne, L., & Lindberg, B. (1975). Structure of extracellular polysaccharide from *Xanthomonas campestris*. *Carbohydrate Research*, *45*(DEC), 275L 282.

Kool, M. M., Schols, H. A., Delahaije, R. J. B. M., Sworn, G., Wierenga, P. A., & Gruppen, H. (2013). The influence of the primary and secondary xanthan structure on the enzymatic hydrolysis of the xanthan backbone. *Carbohydrate Polymers*, *97*(2), 368–375.

Kühnel, S., Schols, H., & Gruppen, H. (2011). Aiming for the complete utilization of sugar-beet pulp: Examination of the effects of mild acid and hydrothermal pretreatment followed by enzymatic digestion. *Biotechnology for Biofuels*, *4*(1), 1–14.

Leijdekkers, A. G. M., Sanders, M. G., Schols, H. A., & Gruppen, H. (2011). Characterizing plant cell wall derived oligosaccharides using hydrophilic interaction chromatography with mass spectrometry detection. *Journal of Chromatography A*, *1218*(51), 9227–9235.

Morris, E. R., Rees, D. A., & Young, G. (1977). Order disorder transition for a bacterial polysaccharide in solution. A role for polysaccharide conformation in recognition between *Xanthomonas* pathogen and its plant host. *Journal of Molecular Biology*, *110*(1), 1–16.

Morrison, N. A., Clark, R., Talashek, T., & Yuan, C. R. (2004). New forms of xanthan gum with enhanced properties. In P. A. Williams, & G. O. Phillips (Eds.), *Gums and stabilisers for food industry* (vol. 12) (pp. 124–130). Cambridge: RSC.

Pelletier, E., Viebke, C., Meadows, J., & Williams, P. A. (2001). A rheological study of the order–disorder conformational transition of xanthan gum. *Biopolymers*, *59*, 339–346.

Peters, H. U., Suh, I. S., Schumpe, A., & Deckwer, W. D. (1993). The pyruvate content of xanthan polysaccharide produced under oxygen limitation. *Biotechnology Letters*, *15*(6), 565–566.

Remoroza, C., Cord-Landwehr, S., Leijdekkers, A. G. M., Moerschbacher, B. M., Schols, H. A., & Gruppen, H. (2012). Combined HILIC–ELSD/ESI–MS^n enables the separation, identification and quantification of sugar beet pectin derived oligomers. *Carbohydrate Polymers*, *90*(1), 41–48.

Renou, F., Petibon, O., Malhiac, C., & Grisel, M. (2013). Effect of xanthan structure on its interaction with locust bean gum: Toward prediction of rheological properties. *Food Hydrocolloids*, *32*(2), 331–340.

Shatwell, K. P., Sutherland, I. W., & Ross-Murphy, S. B. (1990). Influence of acetyl and pyruvate substituents on the solution properties of xanthan polysaccharide. *International Journal of Biological Macromolecules*, *12*(2), 71–78.

Smith, C. J. H., Symes, K. C., Lawson, C. J., & Morris, E. R. (1984). The effect of pyruvate on xanthan solution properties. *Carbohydrate Polymers*, *4*, 153–157.

Stankowski, J. D., Mueller, B. E., & Zeller, S. G. (1993). Location of a second *O*-acetyl group in xanthan gum by reductive-cleavage method. *Carbohydrate Research*, *241*(1), 321–326.

Sutherland, I. W. (1981). Xanthomonas polysaccharides: Improved methods for their comparison. *Carbohydrate Polymers*, *1*(2), 107–115.

Sutherland, I. W. (1984). Hydrolysis of unordered xanthan in solution by fungal cellulases. *Carbohydrate Research*, *131*(1), 93–104.

Tako, M., & Nakamura, S. (1984). Rheology properties of deacetylated xanthan in aqueous-media. *Agricultural and Biological Chemistry*, *48*(12), 2987–2993.